ACS OMEGA

http://pubs.acs.org/journal/acsodf

Article

Interfacial Interactions of a Myoglobin/DOPC Hybrid System at the Air−Water Interface and Its Physicochemical Properties

Ikbal Ahmed, Nilanjan Das, A. K. M. Maidul Islam,* Jasper Rikkert Plaisier, Pietro Parisse, and Jayanta Kumar Bal*

Cite This: *ACS Omega* 2023, 8, 30199−30212

Read Online

ACCESS | Metrics & More | Article Recommendations | Supporting Information

ABSTRACT: In the present study, the intermolecular interactions between a water-insoluble phospholipid (DOPC) and water-soluble protein (myoglobin) and the interaction among themselves were investigated at the air−water interface using the Langmuir and Langmuir−Blodgett techniques. The effects of changes in physicochemical factors, like pH and temperature, on these interactions were also examined. Surface pressure−molecular area (π−A) isotherms of the DOPC monolayer at the air−water interface, with and without myoglobin (Myo) revealed the evolution of various physical properties, such as elastic, thermodynamic, and hysteric properties, in response to changes in subphase pH and temperature. With the increment of subphase pH from 5 to 7 at a fixed temperature (20 °C), the DOPC isotherm expanded, and the in-plane elasticity (C_S^{-1}) decreased, but no significant presence of hysteresis was encountered in either of the pH values. On the other hand, a diminution of temperature (from 20 to 5 °C) leads to an expansion of monolayers yielding low elasticity and significant hysteresis. The incorporation of Myo molecules within the DOPC monolayer decreased the C_S^{-1} value of the DOPC monolayer. Such a decrement in C_S^{-1} was also encountered while increasing the pH and decreasing the temperature (T) of the subphase in the absence of Myo. Systematic expansion of DOPC isotherm and increased hysteric area with the increase in Myo proportion were observed and the atomic force microscopy (AFM) observations suggested a strong conjugation between Myo and DOPC in the mixed monolayer. The denaturation effect of Myo molecules was studied using AFM at different temperatures. Furthermore, the Myo molecules were found to be most surface active at pH = 7, which is very close to its isoelectric point. These observations come up with the interaction mechanism between biomolecules under dynamically varied conditions.

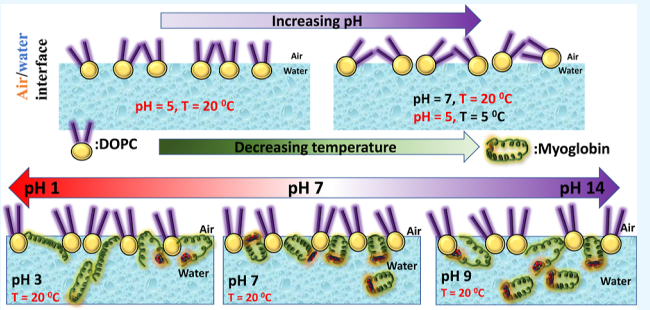

1. INTRODUCTION

The lipid monolayer that forms at the air−water interface can be viewed as a valuable model membrane for studying the interactions of biomolecules, such as DNA, proteins, cellulose, and others, with cell membranes.[1−7] This is because the model membrane mimics the physical and chemical properties of the cell membrane, providing a simplified but representative system for investigating these interactions. Studies of this model membrane have led to a deeper understanding of how biomolecules interact with cell membranes, which is crucial for understanding how cells function and communicate with each other. Additionally, studies of the model membrane have provided insights into biomolecules' fundamental properties and behavior in solution and at interfaces. A particular focus of these studies has been on the role of phospholipids in biological membranes. Due to their unique amphiphilic properties, phospholipids, which are major components of biological membranes,[8] are currently being studied in the fields of biochemistry, chemistry, and polymer science.[9] These studies aim to better understand the structure of phospholipids and how it relates to the biophysical characteristics of biological membranes, as well as the specific molecular interactions of medicinal drugs with biological membranes.[10] Moreover, it is particularly intriguing to observe how phospholipid monolayers spread and develop at the air−water interface because it resembles the physiological function of lung surfactant.[4] Lung surfactant, a crucial component in breathing, comprises phospholipids and determined amounts of surface-active proteins. It works by spreading across the aqueous alveolar−air interface and significantly reducing surface tension, which lessens the effort required for breathing and plays a vital role in controlling pulmonary immunity and other related physiological functions within the lungs.[4] This

Received: April 27, 2023
Accepted: July 31, 2023
Published: August 12, 2023

research has also helped supply the knowledge needed to create synthetic lung surfactants for treating various lung diseases and using phospholipid colloidal dispersions as self-assemblies for drug administration.

However, the properties of the membranes, such as their density, fluidity, and phase transition can be significantly influenced by the hydrocarbon chain length and degree of unsaturation of the constituent phospholipids.[11] A particular membrane need to have the appropriate balance of saturated and unsaturated phospholipids. Interestingly, the most prevalent kind of phospholipids in eukaryotic cells[12] contain the choline group and among them, zwitterionic unsaturated phospholipid, *1,2-dioleoyl-sn-glycero-3-phosphocholine* (DOPC) is of particular interest due to its unique electrostatic and thermodynamic properties.[10] Moreover, being an unsaturated phospholipid, DOPC molecules provide a more fluid state for monolayers, and resemble an excellent natural cell membranes. Its biological and non-toxic characteristics make DOPC a crucial component in producing popular drugs such as morphine sulfate, cytosine, etc.[12] It is also widely used as an emulsifying agent in intravenous nutrition injections.[10] Because of its many uses in biotechnology and potential future applications, DOPC has been the subject of extensive research as a biological model membrane.[3,13] However, despite the widespread use of DOPC, there is a pertaining literature gap of its structural details that originate when intramolecular and intermolecular interactions take place utilizing various forces, like hydrophobic forces, van der Waals (vdW) forces, electrostatic forces, etc.[3,14] Therefore, before designing a drug with DOPC for medicinal usage, it is crucial to thoroughly investigate the interactions between DOPC and other relevant biomolecules such as fatty acids, proteins, vitamins, etc.; understanding these interactions is essential for ensuring the safety and effectiveness of any drug developed using DOPC.

Moreover, understanding the interactions of proteins at the interface of phospholipid structures is important for understanding biological systems and has become a topic of significant interest in various fields, such as biomedical and biochemical research, biosensing, and food science.[1,15] However, the underlying fundamental processes that govern the interfacial dynamics and chemistry between proteins and the surrounding phospholipids are often very complex. Additionally, the detailed lipid−protein interactions, along with their viscoelastic properties (such as compressibility or elasticity) and thermodynamic stability at the interface, have hitherto not been investigated extensively. Early studies demonstrated that when a protein is adsorbed at the air−water interface, it loses its biological activity because of subsequent denaturation or unfolding of the protein.[16−19] However, the mechanisms of these phenomena at the interface are not yet fully understood. Therefore, a model system mimicking a biological membrane environment is utilized to facilitate an in-depth understanding of the intermolecular interactions between proteins and phospholipids at the interface. The study of protein−lipid interactions at an interface can usually be performed in a controlled way by the Langmuir−Blodgett (LB) technique,[20−25] and the Langmuir monolayers[5,26,27] are frequently used as a model system for a better understanding of the interfacial behavior of a protein within a biological system.[28]

Myoglobin is a vital heme protein found in nearly all mammals and the cardiac and skeletal muscle tissues of vertebrates in general.[16,29−31] Moreover, the heme and pigments in Myo are responsible for the color of red meat.[32−34] Myo also works as a potential marker of muscle injury and heart attack in patients with chest pain.[34] Owing to their biological and medicinal importance, understanding the interactions between Myo and the model biomembrane consisting of DOPC is crucial. Studies on myoglobin/DOPC interactions can provide insights into the protein's behavior in biological systems, which can significantly impact the design of treatments for muscle injury, heart attacks, and other related conditions. Additionally, understanding these interactions can also aid in the design of efficient biosensors and other biomedical applications.

In this work, we wish to concentrate on how the DOPC structure and physical properties are altered at the air−water interface by variations in the pH and temperature of its surrounding medium, i.e., the water subphase. Additionally, we will also probe time-dependent adsorption-mediated denaturation and the underlying structural modifications of Myo at different pHs. Finally, we will probe the changes in the DOPC monolayer due to the addition of Myo at the air−water interface at different pHs and temperatures. In other words, the monolayer formed at the air−water interface would be extensively investigated as a useful system to derive microscopic information from macroscopic quantities to elucidate the effects of Myo on the lateral molecular packing in a DOPC membrane. We would particularly be focusing on the molecular level interactions in the pure as well as mixed monolayers at the air−water interface. This information would be helpful in the required knowledge for designing a drug and/or drug delivery agents for practical clinical uses.

2. MATERIALS AND METHODS

2.1. Materials. *1,2-Dioleoyl-sn-glycero-3-phosphocholine* (DOPC) ($M_w \sim 786$ g/mol) and myoglobin (Myo) (extracted from equine heart, $M_w \sim 17$ kDa) were purchased from Sigma-Aldrich Co. and used without further processing. The aqueous solutions of Myo of concentration 5 g/L were prepared using Milli-Q water (resistivity ∼ 18.2 MΩ·cm), and the solutions of DOPC of concentration 1 g/L were prepared by dissolving the DOPC in chloroform. For uniform dissolution, both solutions were held for about 24 h before their usage.

2.2. Surface Pressure−Area Isotherm Study. Surface pressure−area isotherms of pure DOPC, pure Myo, and Myo/DOPC hybrid systems were studied employing a LB trough[14,35] (Apex Instruments, model no. LBXD-NT) of inner working area: 560 mm (L) × 200 mm (W) × 5 mm (H), kept in a neat setting. The LB was made of a PTFE trough with two barriers pushing toward each other. At the central position, a Wilhelmy plate cut from a filter paper with a dimension of 10 × 25 mm^2 was suspended and dipped into the aqueous phase to measure the change in surface tension represented as surface pressure (mN/m). Before the isotherm studies, the LB trough was meticulously cleaned with water purified with a Milli-Q system and then ethanol, followed by purified water for the trough to be dust-free. The surface pressure−area isotherms of pure Myo and pure DOPC were carried out by spreading individual solutions of Myo and DOPC onto the water surface with utmost precision. For the mixed monolayer studies at different mole fractions of Myo and/or DOPC, 30 μL of DOPC was spread gently at the top of the water subphase, and then, three different volumes (1500, 2250, and 3000 μL) of Myo solution were added to it. The solvents were added drop-

https://doi.org/10.1021/acsomega.3c02909
ACS Omega 2023, 8, 30199−30212

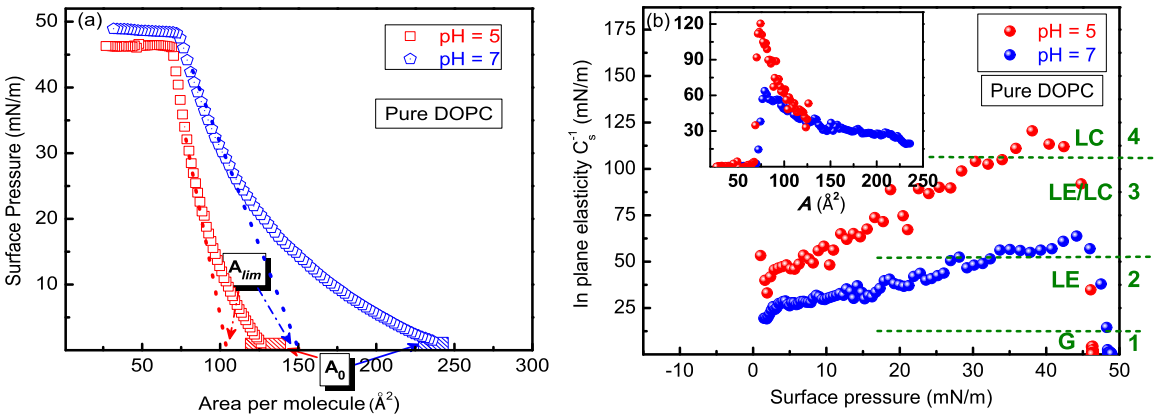

Figure 1. (a) Surface pressure (π)−area/molecule (A) isotherms of pure *1,2-dioleoyl-sn-glycero-3-phosphocholine* (DOPC) as a function of pH recorded at subphase temperature of 20 °C. Extrapolated dotted lines to zero pressure axis display A_{lim} values, whereas the shaded box regions display A_0 values. (b) Corresponding in-plane elasticity (C_S^{-1}) plots with surface pressure (π) and area/mol (A) (shown in the inset).

Table 1. Parameters Calculated by Analyzing Surface Pressure (π)−Area/Molecule (A) Isotherm of Pure DOPC at Different pHs and Temperatures (T)

subphase		A_0 (Å^2)	A_{lim} (Å^2)	$A_0 - A_{lim}$ (Å^2)	A_{cr} (Å^2)	C_S^{-1} (mN/m)	phase
pH	5 (T = 20 °C)	126	104	22	106	120	LE + LC
	7 (T = 20 °C)	237	150	87	74	65	LC
T	5 °C (pH = 5)	296	166	130	62	33	LC
	20 °C (pH = 5)	126	104	22	106	120	LE + LC

by-drop between the two movable surface barriers employing a Hamilton syringe of precision 2.5 μL. Next, the monolayer compression was started after 15 min for the solvent to evaporate and to stabilize the surface pressure (π). The controlled compression yielded surface pressure (mN/m) versus area per molecule (Å^2) (π−A) isotherm. A barrier compression speed of 5 mm/min (corresponds to a change of area = 1000 mm^2/min) was maintained for all the isotherm recordings, and the surface pressure−area isotherms were recorded until it collapsed at a certain pressure, identified as collapse pressure (π_c). The subphase water temperature was controlled with a chiller (First Source Company), whereas the pH was controlled using NaOH and HCl. Moreover, the hysteresis cycle was recorded by subsequent compression and expansion of the available surface area with the moving barrier at a fixed rate of 5 mm/min. Finally, we also confirmed the reproducibility of the isotherm studies, which are scientifically validated.

2.3. LB Film Deposition Method. The monolayers of pure DOPC, pure Myo, and Myo/DOPC mixtures were deposited on hydrophobic Si(100) surfaces at the surface pressure, π = 40 mN/m. The depositions were carried out with two strokes (down-up), starting from the top of the subphase. Moreover, the dipping and lifting speed were kept at a constant value of 5 mm/min. Prior to LB deposition, the substrates were cleaned with RCA to make them hydrophilic and subsequently were treated with hydrofluoric acid (HF) to make them hydrophobic.[14] In RCA cleaning, the Si surfaces were made hydrophilic by adding the hydroxyl group (OH) after boiling them for 10 min at 100 °C in a solution of Milli-Q water ($H_2O/NH_4OH/H_2O_2$ = 2:1:1, by volume), ammonium hydroxide (NH_4OH, Sigma-Aldrich, 25%), and hydrogen peroxide (H_2O_2, Acros Organics, 39%). HF acid treatment hydrophobicized the hydrophilic substrates that had undergone RCA cleaning. Here, the substrates were vertically submerged in HF (10%, 20 mL) solution for 3 min, followed by Milli-Q washing and drying before film deposition.

2.4. AFM Imaging. We have characterized the LB films of pure DOPC, pure Myo and Myo/DOPC mixture deposited at a surface pressure (π) = 40 mN/m on Si(100) substrates with a Solver Pro instrument (NT-MDT) to gather the surface morphology of the films, and scans of 10 × 10 μm^2, 5 × 5 μm^2 and 2 × 2 μm^2 were carried out over various regions of the films for various scan areas. To reduce tip-induced surface alteration, atomic force microscopy (AFM) pictures were taken in ambient circumstances in semi-contact mode using a silicon cantilever (dimensions: 125 μm × 30 μm, spring constant = 42 N/m, resonance frequency = 320 kHz) and a pointed needle-like tip (radius of curvature < 10 nm). The software Gwyddion was used to process and analyze images.

3. RESULTS AND DISCUSSION

3.1. Surface Pressure−Area/Molecule Isotherms of Pure DOPC: Role of Subphase pH. The surface pressure (π)−area (A) isotherms of pure DOPC recorded at two different subphase pH values, i.e., 5 and 7, keeping the temperature constant at T = 20 °C are depicted in Figure 1a. There is a clear shift toward a higher area/molecule with the increase in pH. In addition, the slope of the curve becomes less stiff with the rise in pH. The compression starts at a high A value, and as pressure builds up, A starts decreasing according to molecular interaction and subphase conditions. The lift-off area (A_0) signifies the region where the intermolecular interaction becomes significant, and the DOPC molecules start transforming into a liquid expanded state from a gaseous state. A_0 values for pH 5 and pH 7 are found to be 126 and 237 Å^2 (the values are tabulated in Table 1), respectively. In the LE phase, as A decreases and π increases, the DOPC molecules gradually reorient themselves to a vertical position at the interface, as observed for other phospholipids.[13] However, the

https://doi.org/10.1021/acsomega.3c02909
ACS Omega 2023, 8, 30199−30212

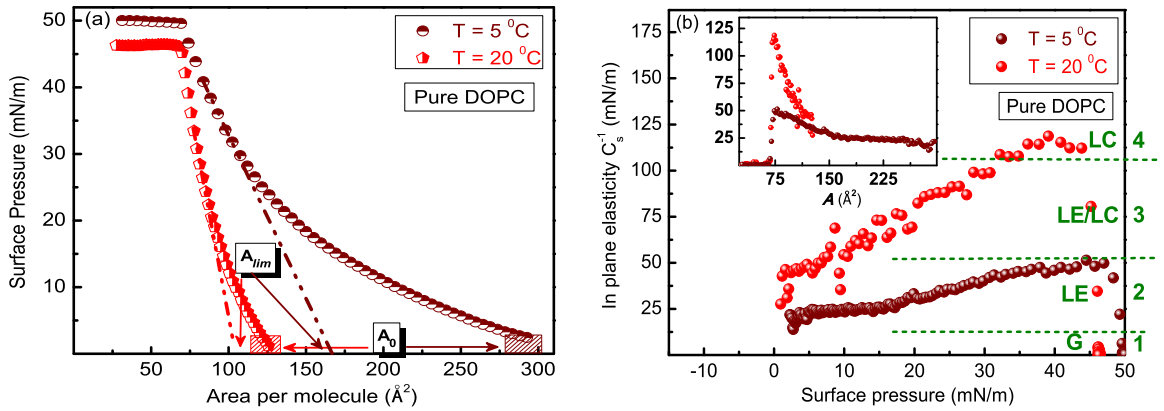

Figure 2. (a) Surface pressure (π)−area/molecule (A) isotherms of pure *1,2-dioleoyl-sn-glycero-3-phosphocholine* (DOPC) as a function of temperature (T) recorded at a constant subphase pH of 5. Extrapolated the dotted lines to zero pressure axis display A_{lim} values, whereas the shaded box regions display A_0 values. (b) Corresponding in-plane elasticity (C_S^{-1}) plots with surface pressure (π) and area/mol (A) (shown in the inset).

unsaturation of hydrocarbon chains of DOPC molecules weakens the vdW cohesive interactions and subsequently reduces the molecular packing in the lipid monolayer.[4] When extending the linear condensed part of the surface pressure−area isotherms toward the area/molecule axis (X-axis), we obtain an area of 104 and 150 Å^2 for pH values of 5 and 7, respectively, and this concerned area is known as the limiting area (A_{lim}). Interestingly, a reported theoretical area of the DOPC hydrophilic headgroup is ∼112 Å[2,36,37] which is utterly close to the A_{lim} value at pH 5. This fact proves the reliability of our isotherm measurements. Following the existing literature,[10] similar collapse pressures, such as 46 and 48 mN/m, are obtained at pH = 5 and 7, respectively. Although all the surface pressure−area isotherms were recorded keeping the spreading volume (30 μL) and solution concentration (5 g/L) the same, a systematic increase in A_0 and A_{lim} value is observed, when the pH of the subphase was increased from 5 to 7. As the vdW force is not affected by pH,[11] perhaps the electrostatic interaction is responsible for this variation. The isoelectric point (IEP) of DOPC is found to be in the pH range of 4−5,[38,39] so the zwitterionic DOPC molecules are essentially neutral at a pH of 5 contrary to a negative value at the pH of 7. Hence, the negatively charged DOPC molecules sense a repulsive force among themselves at the elevated pH value that leads to higher A_0 and A_{lim} values. Moreover, this repulsive electrostatic force hinders the molecular packing of DOPC molecules, causing a decrease in stiffness at the pH of 7. Notably, as the DOPC molecules contain a cis double bond on the acyl chain, it hinders molecular film packing and subsequently, the phospholipids orient themselves in a tilted position over the subphase.[10]

Typically, when the solution is dispersed across the subphase, the phase where the molecules are most distant from one another is known as the gas phase (G). In the course of compression, molecules start interacting with each other, which manifests in the gradual rise of surface pressure. This implies a phase change from the gas phase (G) to the expanded liquid phase (LE). The liquid condensed phase (LC) results from additional compression, which is followed by the solid condensed phase (C). These phases can be identified from the values of static elasticity or compressional modulus (C_S^{-1}). Davies[40] states that the C_S^{-1} values for the gas (G), liquid expanded (LE), liquid expanded/liquid condensed coexistence (LE/LC), liquid condensed (LC), and condensed (C) phases are, respectively, 0−12.5, 12.5−50, 50−100, 100−250, and >250 mN/m. In the C_S^{-1} versus π plots (shown in Figure 1b), these regimes are labeled as 1, 2, 3, and 4, separated by horizontal dashed lines. The following equation can be used to compute the C_S^{-1} from the π−A isotherms[14,35,41,42]

$$C_S^{-1} = -A\left(\frac{\partial \pi}{\partial A}\right)_T \quad (1)$$

where A is the area/molecule at a certain surface pressure π. The stiffness of the isotherm curves is represented by in-plane elasticity, which also displays differences in the physical state of monolayers and aids in understanding the molecular organization. In our study, the peak values of C_S^{-1} (tabulated in Table 1) are observed to be 120 and 65 mN/m for pH = 5 and 7, respectively. Hence, the reduction in subphase pH leads to a higher C_S^{-1} value, and hence, the molecular state of DOPC molecules switch to the LC state (at pH = 5) from the LE/LC state (at pH = 7). This suggests that in a neutral environment (at pH = 7), the DOPC molecules become less condensed, probably due to the acting repulsive electrostatic interactions among the negatively charged DOPC molecules. The A value (see Table 1), at which the highest C_S^{-1} value is found, is known as the critical area (A_{cr}, values are shown in Table 1). This is where the molecules reach their super compressed state, and over-compression may lead to film collapse.[14]

3.2. Surface Pressure−Area/Molecule Isotherms of Pure DOPC: Role of Subphase Temperature. After observing the interesting results of DOPC molecules behaving in different ways in basic and acidic mediums, we further extended our study of the surface pressure−area isotherms at two different temperatures (T = 20 and 5 °C), keeping subphase pH at 5. Figure 2a shows that at T = 5 °C, the isotherm becomes more expanded and less stiff than the isotherm recorded at 20 °C. A_{lim} value is noted at 104 and 166 Å^2 for 20 and 5 °C, respectively (tabulated in Table 1), whereas the A_0 value is found to be 126 and 296 Å^2 for T = 20 °C and T = 5 °C, respectively. The isotherm at T = 20 °C and T = 5 °C exhibits a surface pressure of 12 and 27 mN/m, respectively, at a particular A = 100 Å^2. This drastic increment in A_{lim} and A_0 value at reduced temperature can be attributed to an increment in surface pressure and subsequent expansion of the isotherm. Notably, at low temperatures, the attractive

https://doi.org/10.1021/acsomega.3c02909
ACS Omega 2023, 8, 30199−30212

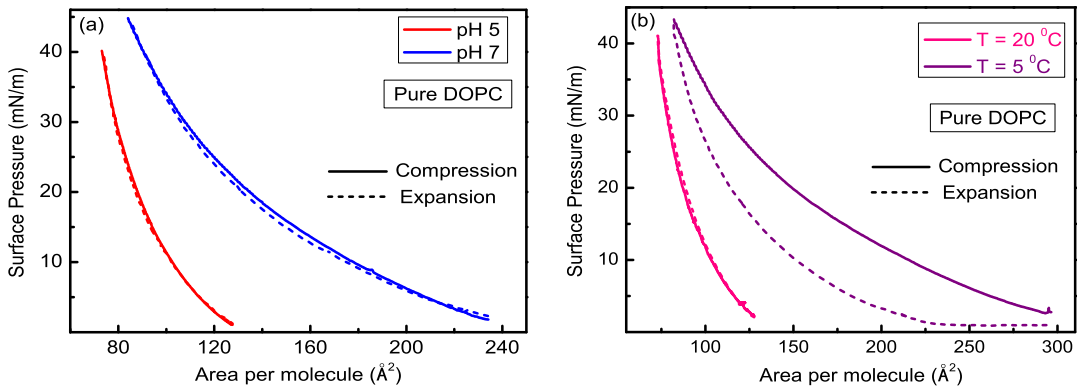

Figure 3. (a) Hysteresis study (compression−decompression) of pure DOPC with varying pH at a subphase temperature (T) of 20 °C and (b) with the varying temperature at a subphase pH = 5.

vdW force acting among the hydrocarbon chains becomes prominent;[2] this attractive vdW force probably causes the DOPC molecules to reorient in a tilted position at T = 5 °C, leading to a shift of the isotherm toward a higher area.

Additionally, the calculated C_S^{-1} values are plotted as a function of π and A (shown in Figure 2b and inset, respectively). The peak C_S^{-1} values in our experiments are found to be 120 and 53 mN/m (shown in Table 1) for surface pressure−area isotherms recorded at T = 20 °C and T = 5 °C, respectively. This shows a reduction in the C_S^{-1} value with the decrease in temperature and implies a decreased surface activity of DOPC molecules at the air−water interface at lower temperatures. The surface activity of molecules at the air−water interface depends on numerous factors, including the solubility of molecules in water. It is well established that DOPC has very negligible solubility in water (~10^{-10} mol/L).[43] On the other hand, DOPC is an eight-chain phospholipid (C8), and due to its relatively short alkyl chain length, the isotherm is dominated by the polar interaction between the DOPC headgroups and water molecules. Markedly, when the temperature is increased (T = 20 °C), the hydrogen bonds between DOPC headgroups and water molecules break down, consequently increasing the surface activity of DOPC molecules.

3.3. Hysteresis Study of Pure DOPC. When the surface area is changed at a constant rate, the isotherm curves during compression and decompression might not coincide. The difference between these curves is referred to as "hysteresis". Hysteresis is primarily caused by either (1) a permanent or transient change in the structure of the molecules under compression or (2) the expulsion of molecules from the air−water contact (material loss).

Moreover, the reorganization of the monolayer during the area expansion when the molecules spontaneously separate from one another is also affected by viscosity. As they must overcome both lateral viscosity and attractive contact forces while disengaging from one another during the expansion cycle. The molecular assembly is subjected to an external force during compression that results in a reduction in the area accessible, creating a closed-packed structure. However, during decompression, the external tension is eliminated by creating a space where the assembly can be organized in a relaxed manner. The primary distinction between these two processes is that in one, the gaseous state is forced into the condensed state, whereas in the second, the condensed film spontaneously picks a way to return to its gaseous state based on its inherent qualities (including cohesion forces between film molecules). To understand the respreading properties of the compressed Langmuir films, a hysteresis study is crucial.

The surface pressure−area (π−A) hysteresis isotherms of pure DOPC at subphase pH = 5 and 7 and temperatures T = 5 and 20 °C are shown in Figure 3a,b, respectively. As evident from Figure 3a, the compression and expansion curves at pH 5 and pH 7 (keeping temperature fixed at 20 °C) follow almost the same path. So, a very negligible or no hysteresis is present in this case, and hence the hysteresis curves appear reversible, i.e., the DOPC molecules recover their initial configuration (before starting the compression) after completion of the expansion cycle. Moreover, the expansion curves (for both pH 5 and pH 7) reach the same π value as the starting π value of the compression curves. This indicates that no molecule expels to the bulk subphase from the interface during the whole process. On the other hand, the reduction of temperature from 20 to 5 °C at a particular pH (pH = 5) gives rise to large hysteric characteristics (shown in Figure 3b). Here, the expansion curve shifts toward the lower area/molecule and eventually reaches almost zero pressure. This can happen due to several factors, such as molecular loss from the air−water interface into the bulk subphase and/or molecular reorganization at the interface. With the decrease in temperature, the attractive vdW force among the DOPC hydrocarbon chains increases significantly.[2] As a result, during compression, the hydrocarbon chains come closer with increasing π, and some of the DOPC molecules get attached and get fusioned[2] to each other, which do not detach entirely during the expansion. Subsequently, we observe the expansion curve to follow a lower area/molecule path than the compression curve at a reduced temperature. This kind of deviation is not encountered with pH variation at T = 20 °C. This is expected as the vdW force is unaltered by the change in subphase pH.[44,45]

At lower surface pressure, the molecules resemble a gaseous state where they stay apart from each other and with the increase in pressure, the molecules come closer and start interacting significantly. Moreover, the physiological parameters, i.e., T and pH of the subphase also affect the molecular orientation and reorientation at the interface. As different degrees of molecular ordering or disordering are related to changes in entropy, the compression−decompression-induced molecular ordering can be better visualized by calculating the change in entropy (ΔS) during the processes.[46] Subsequently, we have calculated the work of compression (W_{com}), work of

https://doi.org/10.1021/acsomega.3c02909
ACS Omega 2023, 8, 30199−30212

Table 2. Calculated Parameters from Surface Pressure (π)−Area/Mol (A) Hysteresis of Pure DOPC, i.e., Work Done during Monolayer Compression (W_{com}), during Monolayer Expansion (W_{exp}), Entropy (ΔS), Gibb's Free Energy of Spreading (ΔG_S) for Compression, and Expansion for Varying pH and T of the Subphase

parameters		W_{com} (kJ/mol)	W_{exp} (kJ/mol)	ΔS (J mol^{-1} K^{-1})	ΔG_S (compression) (J/mol)	ΔG_S (expansion) (J/mol)
pH	5	4.95	7.86	9.93	45.77	71.37
	7	14.5	14.72	0.75	149.37	147.26
T	5 °C	20.55	11.38	−32.98	205.66	114.32
	20 °C	4.95	7.86	9.93	45.77	71.37

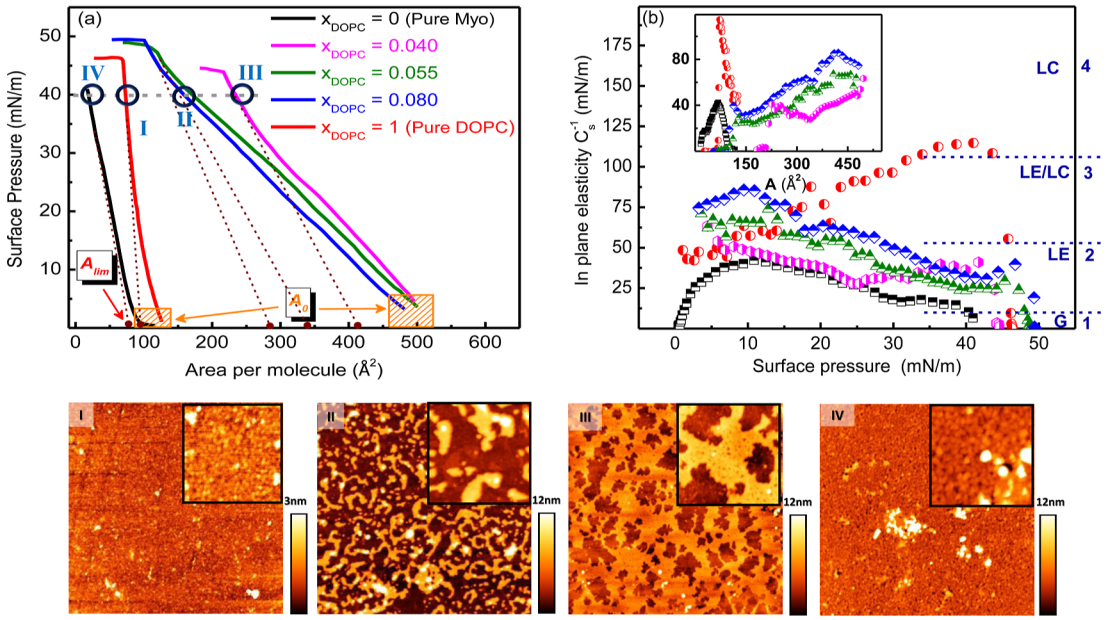

Figure 4. (a) Surface pressure (π)−area/molecule (A) isotherms of pure myoglobin, pure DOPC, and Myo/DOPC mixed systems at different mole fractions of DOPC (X_{DOPC}) at a temperature (T) of 20 °C and subphase pH of 5; and AFM images (dimensions: 5 × 5 μm^2 and inset: 2 × 2 μm^2) of the LB films deposited at 40 mN/m [I: X_{DOPC} = 1 (pure DOPC), II: X_{DOPC} = 0.080, III: X_{DOPC} = 0.040, and IV: X_{DOPC} = 0 (pure Myo)]. (b) Corresponding in-plane elasticity (C_S^{-1}) variation with surface pressure (π) and area/molecule (A) (shown in the inset).

expansion (W_{exp}), change in entropy (ΔS) during the hysteresis study, and Gibb's free energy of spreading (ΔG_S);[35] which are defined as

$$W_{com/exp} = N_A \int_{A_i}^{A_f} \pi \, dA \quad (2)$$

$$\Delta W = W_{exp} - W_{com} \quad (3)$$

$$\Delta S = S_{exp} - S_{com} = \frac{\Delta W}{T} \quad (4)$$

$$\Delta G_S = N_A \int_0^{\pi_0} \pi \, dA \quad (5)$$

where A_i and A_f are the initial and final area/mol respectively and N_A is Avogadro's number and π_o stands for the surface pressure (π) at which we are calculating the Gibbs free energy of spreading. The calculated values of W_{com}, W_{exp}, and ΔS are tabulated in Table 2. Here, we have found W_{exp} to be more than W_{com} at both pHs of 5 and 7 at subphase T = 20 °C and subsequently, we obtained a positive value of ΔS. However, at subphase pH 5 and T = 5 °C, we have found W_{exp} to be less than W_{com} and a negative value of ΔS. We speculate the increment of vdW force at reduced temperature (T = 5 °C) behind this observation.[46] A negative value of ΔS at low temperature (T = 5 °C) signifies that the system has become more ordered[47] than its ordering at elevated temperature (T = 20 °C). We can conclude that after the compression−expansion cycle, the monolayer at T = 5 °C becomes more organized than that recorded at T = 20 °C. Moreover, the positive value of Gibb's free energy of spreading (ΔG_S) for all the monolayers suggests the presence of repulsive interaction among the DOPC molecules at the air−water interface. The elevated value of ΔG_S at pH = 7 at T = 20 °C is due to the increased repulsive interaction among the negatively charged DOPC molecules at this pH value.

3.4. Surface Pressure (π)−Area per Molecule (A) Isotherms of Myo/DOPC Binary Monolayer: Effect of Myoglobin Inclusion. To investigate the effect of Myo insertion on the state of the phospholipid monolayer and to gain more insights into the protein−lipid interaction at the air−water interface, surface pressure−area isotherms of pure myoglobin, and mixed of Myo/DOPC systems with varying DOPC mole fractions (X_{DOPC}) were recorded at subphase pH = 5 and T = 20 °C, as depicted in Figure 4a. The A_{lim} and A_0 values of pure Myo were found to be 77.69 and 114.34 Å^2, respectively. However, the theoretical surface area of Myo (~3626 Å^2)[48] deviates significantly from our empirical A_{lim} value. This can be attributed to the fact that some of the Myo molecules might reside in bulk without affecting the surface pressure. The isotherm of pure Myo shows a monotonous increase in surface pressure with compression. Though highly soluble in water, the Myo molecules show interface activity probably by exposing their hydrophobic parts to the air, and in

https://doi.org/10.1021/acsomega.3c02909
ACS Omega 2023, 8, 30199−30212

Table 3. Calculated Parameters by Analyzing Surface Pressure (π)−Area/Molecule (A) Isotherms of Pure Myo and Myo/DOPC Mixed Systems at Various Mole Fractions of DOPC (X_{DOPC}) at pH = 5 and T = 20 °C

subphase	A_0 (Å^2)	A_{lim} (Å^2)	$A_0 - A_{lim}$ (Å^2)	A_{cr} (Å^2)	C_S^{-1} (mN/m)	phase
X_{DOPC} = 0	114.34	77.69	36.65	69.02	43.25	LE
X_{DOPC} = 0.040	496.97	412.21	84.76	469.23	51.84	LE/LC
X_{DOPC} = 0.055	494.04	338.61	155.43	423.53	65.44	LE/LC
X_{DOPC} = 0.080	480.85	284.66	196.19	422.62	85.77	LE/LC
X_{DOPC} = 1	126	104	22	106	120	LC

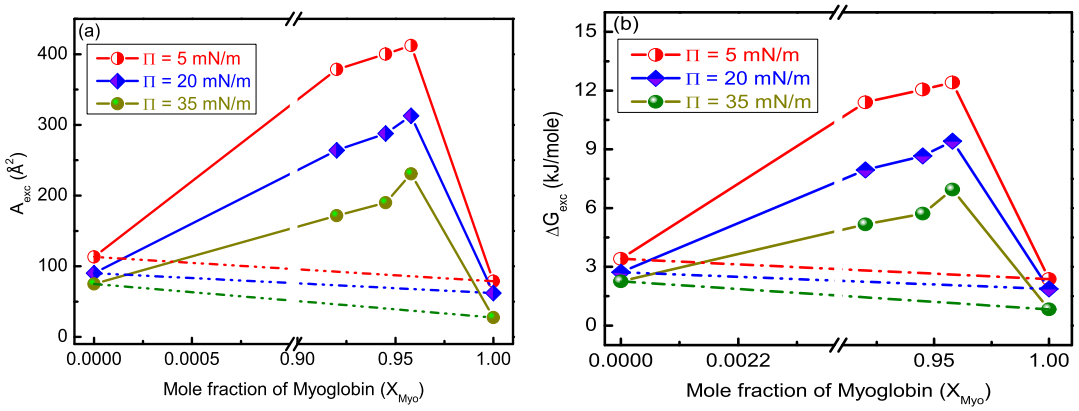

Figure 5. (a) Variation of experimentally determined area/molecule, A_{12} (symbol and continuous solid line), and calculated ideal area/molecule, A_{id} (dash-dotted line) as a function of mole fraction of myoglobin in Myo/DOPC mixed monolayers at three different surface pressures. (b) Evolution of excess Gibb's free energy, ΔG_{exc}, as a function of mole fraction of myoglobin (X_{Myo}) at different surface pressures.

this process, they form an interfacial film that decreases the surface tension. After reaching the maximum surface pressure of 40 mN/m, upon further compression, the collapse is not encountered. Moreover, the stiffness of Myo isotherm was observed to be less compared to pure DOPC isotherm recorded under similar physiochemical conditions. In our experiments, we encountered a systematic increment in A_0 and A_{lim} values with the increment of Myo content in the mixed surface pressure−area isotherms; all the values are tabulated in Table 3. So, the inclusion of Myo makes the monolayer of DOPC more expanded and increases the area per molecule at a particular surface pressure for all the measured mole fractions of DOPC, i.e., X_{DOPC} = 0.040, 0.055, and 0.080. This kind of expansion was also reported for some other similar systems involving phospholipid monolayer,[49−51] and the results are likely to be the effects of increased distance between the lipid hydrophobic chains. Additionally, the slope of the isotherm curves also reduces with the inclusion of Myo into the DOPC monolayer system. The diffusion of Myo from the bulk subphase to the air−water interface and Myo/DOPC interaction, followed by molecular reorientation at the interface are two plausible events in the mixed monolayer system that could explain the current observation. In the mixed system, the hydrophobic and electrostatic interactions between the adsorbed Myo and DOPC molecules modify the orientations of the molecules at the interface with the increase or decrease in π. At a low π value, the Myo molecules orient themselves in a horizontal confirmation to the interface, and with increasing π, they reorient to a more vertical confirmation to the air−water interface. DOPC molecules also tend to follow a similar reorienting trend.

Moreover, to further probe the Myo/DOPC composite system, we have arrested the erstwhile monolayers of pure DOPC (I, Figure 4a), pure Myo (IV, Figure 4a) and Myo/DOPC mixtures [X_{DOPC} = 0.040 (II, Figure 4a), and X_{DOPC} = 0.080 (III, Figure 4a)] from the air−water interface onto solid supported LB films at a surface pressure (π) = 40 mN/m, where the mixed films form a condensed monolayer for its further characterization with AFM. Pure DOPC films were found to be smooth and homogeneous with an RMS roughness (R_{RMS}) value of 0.43 nm (shown in Supporting Information, Table S1). For Myo/DOPC composite films, an inhomogeneous surface with the formation of an island-like structure was noticed, which suggests the possible incorporation of Myo with the DOPC matrix and successful deposition onto Si(100) substrate. Moreover, Myo/DOPC mixed films were found to be rougher than pure DOPC LB films with an increment in surface roughness (R_{RMS}) (shown in Supporting Information, Table S1). On the other hand, the pure Myo LB film has an R_{RMS} = 0.82 nm and a comparable height close to that observed for the film of X_{DOPC} = 0.040. This leads us to speculate the amalgamation of Myo molecules in the mixed Myo/DOPC LB films. Interestingly, the surface coverage increases with the increase of Myo percentage in the mixture (shown in Figure 4a) which agrees with our isotherm observations of strong binding between Myo and DOPC molecules.

Furthermore, to probe into the elastic nature of the mixed system at the air−water interface, in-plane elasticity or compressional modulus (C_S^{-1})[14,35,42,52] was calculated and tabulated in Figure 4b as a function of surface pressure and area/mol (shown in the inset of Figure 4b) for the five different mixtures. Interestingly, the peak C_S^{-1} value increases systematically with an increment of the content of DOPC in the mixed system. The observed peak values of C_S^{-1} are 43.25 and 115.32 mN/m for pure Myo and pure DOPC, respectively, which are the extreme values in our case. Interestingly, the C_S^{-1} value decreases with an increase in the amount of Myo in the mixture; the underlying reason is that the inclusion of Myo makes the DOPC monolayer more

https://doi.org/10.1021/acsomega.3c02909
ACS Omega 2023, 8, 30199−30212

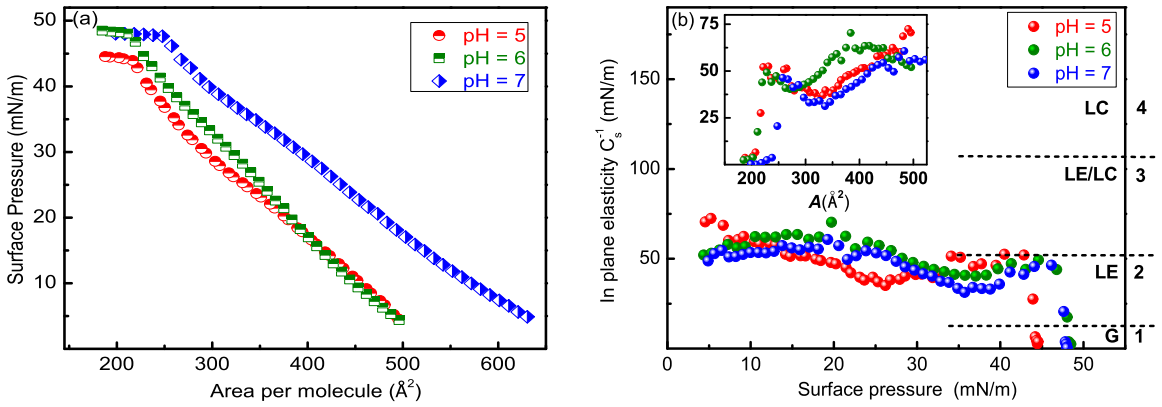

Figure 6. (a) Surface pressure (π)−area/molecule (A) isotherms of Myo/DOPC binary monolayers mixed at a Myo mole fraction of 0.95 (X_{Myo} = 0.95) at a subphase temperature (T) of 20 °C for varying pH of the subphase. (b) Corresponding calculated in-plane elasticity (C_S^{-1}) distribution with surface pressure (π) and area per molecule (A) (shown in the inset).

fluidic and less condensed due to less surface activity at the air−water interface.

3.5. Miscibility of the Mixed Monolayers. To understand how the individual components, i.e., DOPC and Myo, are interacting with each other at the interface in the mixed system, as well as to examine the miscibility of the mixed monolayer components, the excess area per molecule (A_{exc}) was calculated. The A_{exc} is defined in the following way[35,42]

$$A_{exc} = A_{12} - A_{id} \quad (6)$$

where

$$A_{id} = A_{DOPC}X_{DOPC} + A_{Myo}X_{Myo}$$

Here, A_{DOPC} and A_{Myo} are the experimentally determined mean molecular areas of individual pure monolayers, X_{Myo} and X_{DOPC} are the mole fractions of Myo and DOPC, respectively, and A_{12} is the experimentally determined area per molecule from the isotherm of the composite mixture.

For the ideally mixed monolayer, A_{12} follows the ideal curve, a straight line, and a negative or positive deviation from the linearity indicates an attractive or repulsive interaction, respectively. Figure 5a shows a positive deviation of A_{12} from the ideality for three different surface pressures, i.e., π = 5 mN/m, π = 20 mN/m, and π = 35 mN/m. Therefore, it can be concluded that for the studied mole fractions of Myo, there was a noticeable repulsive interaction between the molecules in the mixed monolayer system. This is probably caused by the presence of neutrally charged DOPC (IEP—4−5)[38,39] molecules and positively charged myoglobin (IEP = 7.5)[53] molecules at the subphase pH = 5.

3.6. Energetic Stability of Mixed Monolayers. The interaction between Myo and DOPC can also be analyzed thermodynamically in terms of the excess Gibb's free energy (ΔG_{exc}) at a particular surface pressure for the composite monolayer, and it is defined by the following equation[35,54]

$$\Delta G_{exc} = N_A \int_{\pi^*}^{\pi} A_{exc}\, d\pi \quad (7)$$

where N_A is the Avogadro number, π is the surface pressure at which Gibb's free energy is calculated, and π^* is the pressure where the two components of the mixture behave ideally and, in that situation, ΔG_{exc} = 0. It is noteworthy that π^* is the pressure range where the vapor phase and liquid expanded phases coexist and the region where the pressure rises significantly during compression. Figure 5b depicts the variation of excess Gibb's free energy as a function of mole fractions of Myo at three different surface pressures (5, 20, and 35 mN/m). We observed the positive values of ΔG_{exc} in the entire range of the analyzed mole fraction of Myo, and consequently, the positive departure from the ideality (i.e., ΔG_{exc} = 0), indicating a repulsive interaction between Myo and DOPC in the mixed monolayer system.

3.7. Surface Pressure (π)−Area per Molecule (A) Isotherms of Myo/DOPC Binary Monolayer: Effect of pH. After encountering these peculiar results and since the electrostatic charges of both Myo and DOPC are explicitly dependent on subphase pH and their respective IEPs, we have further extended the π−A isotherm studies of Myo/DOPC mixed system at different subphase pH = 5, 6, and 7. The recorded surface pressure−area isotherms in Figure 6a show a linear increment in π with a decrease in area/mol for all three pH values. Moreover, the area/molecule (A) of the isotherm at pH = 7 is more than surface pressure−area isotherms at pH = 5 and 6. However, the area/molecule of the isotherm at a subphase pH 6 is greater than pH 5 only at higher pressures, i.e., when $\pi \geq$ 20 mN/m. This kind of area/mol expansion of the isotherm strongly depends on the two major acting forces, which are electrostatic force and hydrophobic force.

Interestingly, the electrostatic charges of Myo and DOPC show a strong dependence on subphase pH due to their IEPs of 7.5[53] and 4−5,[38,39] respectively. The effective charges of pure Myo and pure DOPC at different pHs of interest are tabulated in Table 4; all are collected from recently reported works.[38,39,53] In our study of isotherm at pH 7, Myo is neutrally charged, whereas DOPC is negatively charged. As the charge of Myo molecules decreases, it becomes highly surface-active at pH 7, which is very close to its IEP.[53,55] In this physiochemical condition, the intermolecular interactions

Table 4. Dependence of Charge of Pure Myoglobin and Pure DOPC on the pH of Subphase and IEPs of the Molecules

pH value	charge of myoglobin	charge of DOPC
pH = 3	+ve	+ve
pH = 5	+ve	−ve/neutral
pH = 6	+ve	−ve
pH = 7	neutral/+ve	−ve
pH = 9	−ve	−ve

https://doi.org/10.1021/acsomega.3c02909
ACS Omega 2023, 8, 30199−30212

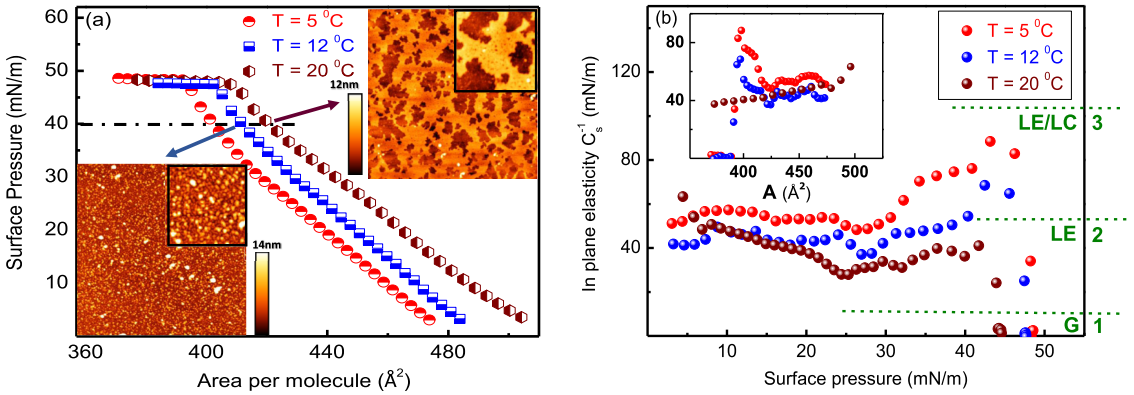

Figure 7. (a) Surface pressure (π)−area/molecule (A) isotherms of Myo/DOPC binary monolayers mixed at the Myo mole fraction of 0.95 (X_{Myo} = 0.95) at a subphase pH = 5 at three different temperatures, T = 5, 12, and 20 °C of the subphase; and AFM images (dimension: 5 × 5 μm^2, inset: 2 × 2 μm^2) of LB films deposited at π = 40 mN/m (bottom left corner corresponds to the film deposited at T = 12 °C and top right corner corresponds to the film deposited at T = 20 °C). (b) Corresponding calculated in-plane elasticity (C_S^{-1}) distribution with surface pressure (π) and area per molecule (A) (shown in the inset).

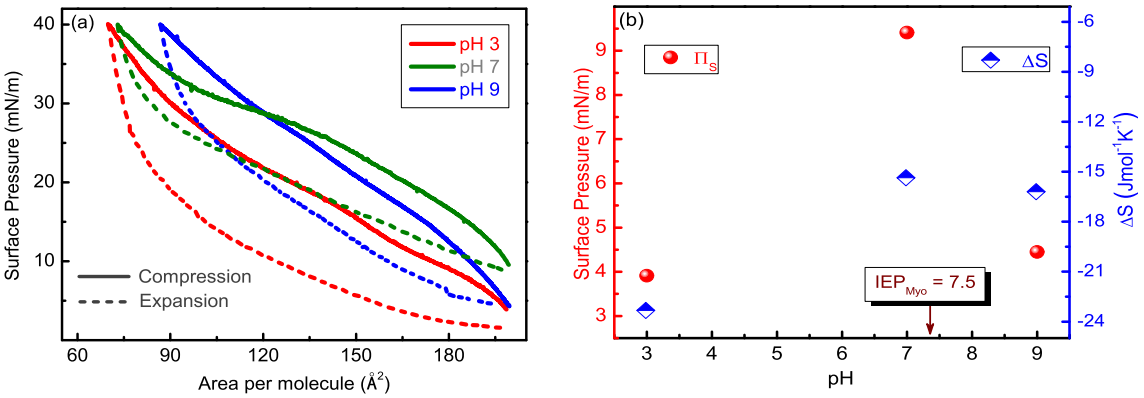

Figure 8. (a) Hysteresis study of the myoglobin/DOPC binary systems mixed at the Myo mole fraction of 0.95 (X_{Myo} = 0.95) recorded at T = 20 °C at three different pH values of the subphase, viz., pH = 3, 7, and 9. (b) Variation of starting surface pressure (π_s) and entropy (ΔS) with the pH of water subphase.

among the neutral Myo molecules, as well as their interactions with water molecules decreases, which results in an increase in its surface activity or adsorption to the air−water interface. Additionally, a repulsive force acting among negatively charged DOPC molecules are also behind the expanded curve at pH 7.

Notably, electrostatic and hydrophobic forces are the two major interplaying forces at the air−water interface here. Hydrophobic forces are widely accepted to act on a length scale where electrostatic interactions are sensed.[56] However, some long-range hydrophobic interactions have also recently been reported.[57−60] To conclude further, we need better theoretical and experimental validation of the aforementioned acting forces. Finally, we have calculated the in-plane elasticity (C_S^{-1}) and plotted it as a function of surface pressure, π in Figure 6b, and area/molecule in the inset of Figure 6b. The peak values of C_S^{-1} were found to be more at pH = 5 than that observed at pH = 7. This is observed probably because, at pH = 5, DOPC has an effective neutral charge (shown in Table 4) and increased surface activity; hence, it increases the C_S^{-1} value at this pH of the subphase. However, pure Myo molecules have a lower C_S^{-1} value than pure DOPC (shown in Figure 4b) and do not contribute much to the C_S^{-1} value of the mixed system, although being neutral at pH = 7. Moreover, surface pressure-dependent molecular orientation/reorientation also plays a major role in the characteristics of the isotherm. At low pressure, probably at a range of π = 0−10 mN/m, the Myo molecules orient themselves horizontally at the air−water interface forming a plane sheet-like structure similar to those recently reported for other globular proteins.[61] Afterward, with the increase in surface pressure, the molecules gradually reorient to a vertical position and reach a nearly vertical orientation at a range of π = 30−40 mN/m. DOPC molecules also resemble a similar trend with little different isothermal characteristics. Thus, the isotherm characteristics also strongly depend on the molecular orientation of the individual components spread onto the air−water interface.

3.8. Surface Pressure (π)−Area per Molecule (A) Isotherms of Myo/DOPC Binary Monolayer: Effect of Subphase Temperature. After unveiling these interesting interactions between Myo and DOPC at the air−water interface at different subphase pHs, we decided to probe the mixed system at different temperatures of interest to elucidate the thermodynamic properties of the interaction-mediated molecular orientation/reorientation at the interface. The recorded surface pressure−area isotherms at a Myo mole fraction, X_{Myo} = 0.94, and subphase pH = 5 at three different temperatures (T = 5, 12, and 20 °C) are represented in Figure 7a. As evident, the isotherm is expanded (shifted toward increasing the area/molecule) with the increase in temperature.

https://doi.org/10.1021/acsomega.3c02909
ACS Omega 2023, 8, 30199−30212

The expansion can be attributed to the denaturation of myoglobin at elevated temperatures. It is well established that Myo molecules are denatured to a high extent at low temperatures at a pH = 5 and due to this unfolding caused by acidic subphase, the hydrodynamic volume of Myo molecules increases.[62,63] On top of that, with the increase in temperature, the denaturation of Myo is accelerated and this causes more activity of the molecules at the air−water interface expanding the mixed surface pressure−area isotherms at higher temperatures. Surprisingly, the AFM analysis of the LB film deposited at π = 40 mN/m of the Myo/DOPC mixture (X_{Myo} = 0.95) at T = 12 °C suggests a retained globular protein structure of the Myo molecules inside the DOPC matrix (shown in Figure 7a, bottom left). However, the LB film of the Myo/DOPC mixture at T = 20 °C was found to be rigorously denatured on the solid supported LB films. The decreased height of the film deposited at T = 12 °C confirms this argument as denaturation would decrease the film height and form a plane sheet-like structure.[64]

Additionally, the variation of the calculated in-plane elasticity (C_S^{-1}) values with surface pressure (π) (shown in Figure 7b) and area/mol (A) (shown in the inset of Figure 7b) suggests an increment of C_S^{-1} with the temperature. We speculate that the increment in temperature denatures the Myo molecules and makes the mixed system more fluidic or less elastic. Contrarily, at low temperatures, we observe a greater C_S^{-1} value for less denaturation of Myo molecules.

3.9. Progressive Hysteresis Study of Myo/DOPC Mixed Monolayer: Effect of Subphase pH. To unveil the role of molecular interactions behind the reorientation of Myo and DOPC at the interface, and to find, if there is any molecular loss from the air−water interface to the bulk subphase, we have further probed the hysteresis behavior of the Myo/DOPC mixed system at T = 20 °C at pH = 3, 7, and 9. The results are shown in Figure 8a. As can be seen, there is the existence of hysteresis at all the different values of pHs. However, the enclosed hysteresis areas are not the same in all cases; the hysteresis curve at pH = 3 has the maximum enclosed area inside it compared to the other pH values. Notably, DOPC molecules did not show any hysteresis (as shown in Figure 3a) at subphase pHs of 5 and 7; hence, we can presume that Myo molecules contribute primarily to the hysteresis curve, but there could be an effect of molecular reorientation due to the presence of DOPC molecules at the interface. This presumption is also backed by our hysteresis study of pure myoglobin molecules at pH = 5 and T = 20 °C, where we found an increment in the enclosed hysteresis area with an increased volume of Myo at the subphase (shown in Supporting Information, Figure S3a).

Interestingly, in Figure 8a, all the expansion curves return to their initial values of surface pressure (π), which were encountered when starting the respective compression cycles, indicating that neither Myo nor DOPC molecules were lost from the interface into the bulk during the hysteresis processes. Additionally, the slope of the compression curves also varies at different pH values, and it seems that the compression curve at pH = 7 has a smaller slope than pH = 3 and 9; which is more pronounced at high surface pressures (after π = 30 mN/m). This observation is backed by our study of in-plane elasticity (C_S^{-1}; which essentially denotes the slope of the isotherm) variation with surface pressure (π) (shown in Figure 6b), where we have found the peak values of C_S^{-1} were more at pH = 5 than that observed at pH = 7. The reason was concluded as a smaller contribution of water-soluble Myo molecules to C_S^{-1} value in comparison to DOPC despite the high surface activity of Myo at pH = 7.

Additionally, the surface pressure when starting the compression process of the hysteresis curve, also known as the starting surface pressure (π_s), is highest at pH = 7 than at pH = 3 and 9, are depicted in Figure 8b (left side scale, red plots). This happens because of the higher surface activity of Myo molecules near its IEP (pH = 7.5). At this pH value, the Myo molecules are neutrally charged and hence have a minimal interaction among themselves and DOPC and the water molecules;[47] as a result, they are most surface-active at this pH value. On the other hand, the surface activity of Myo molecules decrease at pH = 3 and 9 due to the possession of positive and negative charges, respectively, which increase the intermolecular interactions between Myo/DOPC, Myo−water, and Myo molecules. Notably, Myo denaturation at the air−water interface is also pH-dependent, and the structural changes of Myo molecules are caused by denaturation at different pH values have been well documented in the literature.[18,65] Therefore, the involvement of denaturation-induced molecular reorientation at the interface also strongly affects the observed qualitative parameters.

Since different degrees of ordering−disordering are explicitly correlated to molecular reorganization at the air−water interface, we have calculated the change in entropy (ΔS) of the mixed system that is depicted as a function of pH in Figure 8b (right scale, blue plots). We have encountered ΔS = −23.33, −15.36, and −16.20 J mol^{-1} K^{-1} for pH = 3, 7, and 9, respectively. It indicates that the Myo/DOPC mixture becomes most ordered during the hysteresis cycle at pH = 3; interestingly, at this pH value, both Myo and DOPC molecules are positively charged (shown in Table 4). These positive charges likely lead to significant interactions between both Myo and DOPC molecules and the surrounding water molecules, resulting in the observed reorientation to the most ordered assembly at the air−water interface. The calculated values of Gibb's free energy of spreading (ΔG_S) show positive values (shown in Table 5) at pH = 3, 7, and 9 indicating the presence of repulsive interactions between Myo and DOPC molecules at all the pH values.[35] The denaturation of Myo can also explain these peculiar phenomena at various pHs. Myo molecules are less denatured at pH 7, whereas it is highly denatured at pH = 3.[66] Acid denaturation of Myo happens from the histidyl group that is masked inside the native protein. Dropping the pH from 5 to 4 causes a loss of 50% of the helical structure[67] of Myo molecules. The conformation of myoglobin at reduced pH is far from the protein's native structure,[67] and the viscosity of Myo increases in acidic environments.[62] Moreover, a decreasing surface

Table 5. Calculated Gibbs Free Energy of Spreading (ΔG_S) during Compression and Expansion Cycles from the Surface Pressure (π)−Area/Molecule (A) Hysteresis Studies of Myo/DOPC Mixtures at the Myo Mole Fraction of 0.95 (X_{Myo} = 0.95) Recorded at T = 20 °C at Three Different pH Values of the Subphase, i.e., pH = 3, 7, and 9

pH	ΔG_S (compression) (J/mol)	ΔG_S (expansion) (J/mol)
3	151.83	−81.79
7	193.75	−147.62
9	155.33	−105.04

https://doi.org/10.1021/acsomega.3c02909
ACS Omega 2023, 8, 30199−30212

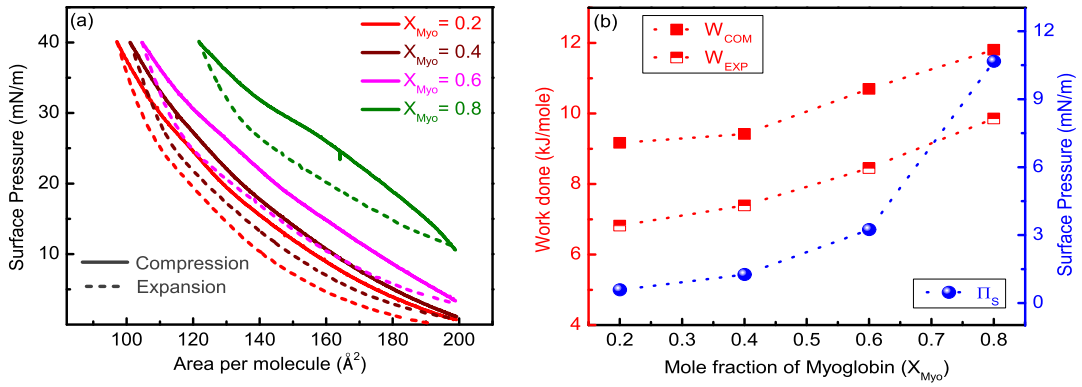

Figure 9. (a) Hysteresis studies of the myoglobin/DOPC mixtures at four-mole fractions of myoglobin (X_{Myo}), viz., X_{Myo} = 0.2, 0.4, 0.6, and 0.8 recorded at subphase pH = 5 and T = 20 °C. (b) Variation of work done of compression (W_{com}), work done of expansion (W_{exp}), and starting surface pressure (π_s) with X_{Myo}.

Table 6. Calculated Parameters from Surface Pressure (π)−Area/Molecule (A) Hysteresis Studies of Myo/DOPC Mixtures at X_{Myo} = 0.2, 0.4, 0.6, and 0.8., viz., Work Done during Monolayer Compression (W_{com}), during Monolayer Expansion (W_{exp}), and Entropy (ΔS) at pH = 5 and T = 20 °C

mole fraction of myoglobin	W_{com} (kJ/mol)	W_{exp} (kJ/mol)	ΔS (J mol^{-1} K^{-1})	ΔG_S (compression) (J/mol)	ΔG_S (expansion) (J/mol)
0.2	9.17	6.82	−7.83	91.73	−68.18
0.4	9.42	7.39	−6.76	94.25	−73.96
0.6	10.70	8.45	−7.50	107.03	−84.50
0.8	11.81	9.86	−6.5	118.17	−98.66

activity of Myo was observed when the subphase pH was decreased to 3 from its IEP of pH = 7.5.[53] Researchers also concluded that Myo reaches a molten globular state when denatured. The molten globule state is an intermediate state of protein folding when the secondary structure is intact, but the tertiary rigid structure is broken or deformed. In this state, it has hydrophobic patches which are accessible to the solvent and has 1.5 times more hydrodynamic volume than its native state.[62]

3.10. Progressive Hysteresis Study of Myo/DOPC Mixed Monolayer: Effect of Myoglobin Mole Fraction. We have presented the hysteresis cycles at four different myoglobin mole fractions, X_{Myo} = 0.2, 0.4, 0.6, and 0.8 in Figure 9a, and a clear presence of hysteresis is there for all the studied mole fractions of myoglobin. However, all the expansion curves reach the starting value of surface pressure at the expansion end, which was found when starting the compression curves, and this tells that there is no molecular loss of Myo or DOPC from the interface during the hysteresis processes; this kind of hysteretic behavior is known as reversible hysteresis. Similar kinds of reversible hysteresis behaviors were also encountered in the case of pure myoglobin studied at the subphase pH = 5 and T = 20 °C (Supporting Information, S3); but not in the case of pure DOPC studied under the same physiochemical conditions. This helps us to conclude with the fact that the origin of hysteresis in the case of Myo/DOPC mixed hysteresis results is preliminarily due to the presence of myoglobin molecules in the mixture. Interestingly, the work done during compression (W_{com}) and expansion (W_{exp}) cycles increases systematically with an increase in the amount of myoglobin in the mixture, as shown in Figure 9b.

During the compression cycle, the mixed isotherm is subjected to decreasing surface area at a constant rate of 10 cm^2/min, and W_{com} work is done during the process where the Myo and DOPC molecules constantly interact and reorient themselves at the air−water interface employing electrostatic and hydrophobic forces. With the increase in surface pressure, both the Myo and DOPC molecules start to reorient to a vertical position at the air−water interface from an erstwhile horizontal position at an initial surface pressure close to π = 0 mN/m. Similarly, during the compression cycle, the surface area of the monolayer is reduced at the cost of work of W_{exp}; all the calculated values of W_{exp}, W_{com}, and ΔS are shown in Table 6. Certainly, during either of the processes, Myo and DOPC molecules constantly change their conformation by reorienting at the air−water interface. Moreover, we observed a systematic increase in starting surface pressure with an increment of myoglobin mole fraction (X_{Myo}) in the mixture, as depicted in Figure 9b. This signifies that the presence of myoglobin strongly affects the starting surface pressure (π_S), probably due to surface adsorption and incomplete denaturation of myoglobin[18,53,67] in correlation with our kinetic study of pure myoglobin (shown in Supporting Information, S1). Furthermore, the calculated positive value of Gibb's free energy of spreading (ΔG_S) shows the presence of repulsive interactions between Myo and DOPC molecules at all the mole fractions of Myo (X_{Myo}) and the ΔG_S value (shown in Table 6) increases with X_{Myo} during the compression and expansion cycles of the hysteresis studies. Interestingly, during the denaturation process, the Myo molecules start exposing their hydrophobic parts to the air gradually because of contact with Myo with air. This kind of exposure of hydrophobic parts of myoglobin and another few globular proteins toward the air surface changes the protein conformation in a significant way.[16] The time-dependent incomplete denaturation of Myo molecules at the air−water interface is a complicated process,[68] and it causes the protein knots to open up, destroying its tertiary structure. Contrary to bulk denaturation of proteins resulting in unfolding to a more open structure, surface denaturation can affect protein spreading at the interface.[21] The detached protein chains accumulate at the interface and

https://doi.org/10.1021/acsomega.3c02909
ACS Omega 2023, 8, 30199−30212

probably form a plane sheet-like structure, as observed for other globular proteins.[61]

4. CONCLUSIONS

This study demonstrated the intermolecular interaction among water-insoluble pure DOPC, water-soluble pure Myo, and Myo/DOPC mixed monolayers at the air−water interface employing π−A isotherm and hysteresis studies varying subphase pH and temperature. The structure and properties of pure DOPC and pure Myo are altered due to changes in pH and temperature of the subphase. The kinetic study (π−t isotherm) of pure Myo suggests a systematic increment of Myo surface activity induced by adsorption-mediated incomplete denaturation of the protein molecules. Moreover, the adsorption of Myo onto the DOPC monolayer decreased the in-plane elasticity of the DOPC monolayer substantially. This decrement in the in-plane elasticity was also vivid at higher pH and lower temperature of the subphase in the absence of Myo molecules. Furthermore, the miscibility study suggests an attractive interaction between Myo and DOPC and the data for Gibb's excess free energy (ΔG_{exc}), indicating that phospholipid monolayers with embedded Myo molecules are thermodynamically stable and agree with the miscibility study. However, we performed the experiments for very low mole fractions of Myo. The incorporation of Myo onto the DOPC monolayers expands the isotherm of DOPC; a similar alteration of the mixed surface pressure−area isotherms is found while increasing the temperature and pH of the subphase. On the other hand, the hysteresis area of the Myo/DOPC mixed system gradually increases with an increment in Myo percentage at the air−water interface, suggesting a strong influence of Myo molecules during molecular orientation/reorientation at the interface. Similarly, the largest value of starting pressure obtained at pH = 7 proposes the utmost surface activity of Myo closer to its IEP point. The adsorption of protein and its denaturation at the air−water interface is a lucrative research topic and is widely studied by researchers.[48,64,68,69] However, a detailed understanding of protein denaturation, molecular reorganization, and structural modification at the air−water interface are still scarce. In this perspective, our studies are of paramount importance in the field of fundamental biophysics and surface−interface physics.

■ ASSOCIATED CONTENT

Supporting Information

The Supporting Information is available free of charge at https://pubs.acs.org/doi/10.1021/acsomega.3c02909.

Surface roughness data obtained from AFM analysis of pure DOPC, pure Myo, and Myo/DOPC composite LB films; kinetic study (π−t) of pure myoglobin; and hysteresis studies of pure myoglobin and Myo/DOPC mixed monolayers at the air−water interface (PDF)

■ AUTHOR INFORMATION

Corresponding Authors

A. K. M. Maidul Islam − *Department of Physics, Aliah University, Kolkata 700160, India;* orcid.org/0000-0002-2224-1142; Email: maidul79@gmail.com

Jayanta Kumar Bal − *Abhedananda Mahavidyalaya, University of Burdwan, Sainthia 731234, India;* orcid.org/0000-0002-1814-1018; Email: jayanta.bal@gmail.com

Authors

Ikbal Ahmed − *Department of Physics, Aliah University, Kolkata 700160, India; International Centre for Theoretical Sciences, Tata Institute of Fundamental Research, Bengaluru 560089, India;* orcid.org/0000-0003-0969-788X

Nilanjan Das − *Abhedananda Mahavidyalaya, University of Burdwan, Sainthia 731234, India*

Jasper Rikkert Plaisier − *Elettra-Sincrotrone Trieste S.C.p.A., Trieste 34149, Italy;* orcid.org/0000-0003-1981-1498

Pietro Parisse − *Elettra-Sincrotrone Trieste S.C.p.A., Trieste 34149, Italy; Istituto Officina dei Materiali—Consiglio Nazionale delle Ricerche, Trieste 34149, Italy*

Complete contact information is available at: https://pubs.acs.org/10.1021/acsomega.3c02909

Notes

The authors declare no competing financial interest.

■ ACKNOWLEDGMENTS

J.K.B. thankfully acknowledge Department of Science and Technology (DST), Government of India, for providing the research grant through SERB (CRG/2018/002290). The financial support received from the DST and ICTP under the IndiaElettra access program to carry out XRR experiments at MCX beamline of Elettra is gratefully acknowledged.

■ REFERENCES

(1) Yun, H. J.; Choi, Y. W.; Kim, N. J.; Sohn, D. W. Physicochemical Properties of Phosphatidylcholine (PC) Monolayers with Different Alkyl Chains, at the Air/Water Interface. *Bull. Korean Chem. Soc.* **2003**, *24*, 377−383.

(2) Pichot, R.; Watson, R.; Norton, I. Phospholipids at the Interface: Current Trends and Challenges. *Int. J. Mol. Sci.* **2013**, *14*, 11767−11794.

(3) Hao, C.; Sun, R.; Zhang, J. Mixed Monolayers of DOPC and Palmitic Acid at the Liquid−Air Interface. *Colloids Surf., B* **2013**, *112*, 441−445.

(4) Guzmán, E.; Liggieri, L.; Santini, E.; Ferrari, M.; Ravera, F. DPPC−DOPC Langmuir Monolayers Modified by Hydrophilic Silica Nanoparticles: Phase Behaviour, Structure and Rheology. *Colloids Surf., A* **2012**, *413*, 174−183.

(5) Jurak, M.; Wiącek, A. E.; Mroczka, R.; Łopucki, R. Chitosan/Phospholipid Coated Polyethylene Terephthalate (PET) Polymer Surfaces Activated by Air Plasma. *Colloids Surf., A* **2017**, *532*, 155−164.

(6) Wiacek, A. E.; Holysz, L.; Chibowski, E. Effect of Temperature on *n* -Tetradecane Emulsion in the Presence of Phospholipid DPPC and Enzyme Lipase or Phospholipase A $_2$. *Langmuir* **2008**, *24*, 7413−7420.

(7) Wiacek, A. E. Effect of Ionic Strength on Electrokinetic Properties of Oil/Water Emulsions with Dipalmitoylphosphatidylcholine. *Colloids Surf., A* **2007**, *302*, 141−149.

(8) Ahmed, I.; Dildar, L.; Haque, A.; Patra, P.; Mukhopadhyay, M.; Hazra, S.; Kulkarni, M.; Thomas, S.; Plaisier, J. R.; Dutta, S. B.; Bal, J. K. Chitosan-Fatty Acid Interaction Mediated Growth of Langmuir Monolayer and Langmuir-Blodgett Films. *J. Colloid Interface Sci.* **2018**, *514*, 433−442.

(9) Gaboriaud, F.; Volinsky, R.; Berman, A.; Jelinek, R. Temperature Dependence of the Organization and Molecular Interactions within Phospholipid/Diacetylene Langmuir Films. *J. Colloid Interface Sci.* **2005**, *287*, 191−197.

(10) Gradella Villalva, D.; Diociaiuti, M.; Giansanti, L.; Petaccia, M.; Bešker, N.; Mancini, G. Molecular Packing in Langmuir Monolayers

Composed of a Phosphatidylcholine and a Pyrene Lipid. *J. Phys. Chem. B* **2016**, *120*, 1126−1133.
(11) Vollhardt, D. Effect of Unsaturation in Fatty Acids on the Main Characteristics of Langmuir Monolayers. *J. Phys. Chem. C* **2007**, *111*, 6805−6812.
(12) Gellert, F.; Ahrens, H.; Helm, C. A. Oxidation of Unsaturated Phospholipids: A Monolayer Study. *Langmuir* **2020**, *36*, 12213−12220.
(13) Yi, P.; Chen, K. L. Interaction of Multiwalled Carbon Nanotubes with Supported Lipid Bilayers and Vesicles as Model Biological Membranes. *Environ. Sci. Technol.* **2013**, *47*, 5711−5719.
(14) Ahmed, I.; Mathur, T.; Islam, A. K. M. M.; Plaisier, J. R.; Parisse, P.; Thomas, S.; Bal, J. K. Structure and Elastic Properties of an Unsymmetrical Bi-Heterocyclic Azo Compound in the Langmuir Monolayer and Langmuir−Blodgett Film. *ACS Omega* **2020**, *5*, 21538−21549.
(15) Stelzle, M.; Weissmueller, G.; Sackmann, E. On the Application of Supported Bilayers as Receptive Layers for Biosensors with Electrical Detection. *J. Phys. Chem.* **1993**, *97*, 2974−2981.
(16) Macritchie, F. Proteins at Interfaces. *Adv. Protein Chem.* **1978**, *32*, 283−326.
(17) Ronzon, F.; Desbat, B.; Chauvet, J.-P.; Roux, B. Penetration of a GPI-Anchored Protein into Phospholipid Monolayers Spread at the Air/Water Interface. *Colloids Surf., B* **2002**, *23*, 365−373.
(18) Andrade, J. D.; Hlady, V.; Wei, A. P.; Ho, C. H.; Lea, A.; Jeon, S.; Lin, Y.; Stroup, E. Proteins at Interfaces: Principles, Multivariate Aspects, Protein Resistant Surfaces, and Direct Imaging and Manipulation of Adsorbed Proteins Biologically Modified Polymeric Biomaterial Surfaces. *Clin. Mater.* **1992**, *11*, 67−84.
(19) Caseli, L.; Oliveira, R. G.; Masui, D. C.; Furriel, R. P. M.; Leone, F. A.; Maggio, B.; Zaniquelli, M. E. D. Effect of Molecular Surface Packing on the Enzymatic Activity Modulation of an Anchored Protein on Phospholipid Langmuir Monolayers. *Langmuir* **2005**, *21*, 4090−4095.
(20) Schwuger, M. Mechanism of Interaction between Ionic Surfactants and Polyglycol Ethers in Water. *J. Colloid Interface Sci.* **1973**, *43*, 491−498.
(21) Chen, H.; Hsu, S. L.; Tirrell, D. A.; Stidham, H. D. A PH Dependent Coil-to-Sheet Transition in a Periodic Artificial Protein Adsorbed at the Air−Water Interface. *Langmuir* **1997**, *13*, 4775−4778.
(22) Wertz, C. F.; Santore, M. M. Adsorption and Relaxation Kinetics of Albumin and Fibrinogen on Hydrophobic Surfaces: Single-Species and Competitive Behavior. *Langmuir* **1999**, *15*, 8884−8894.
(23) Wertz, C. F.; Santore, M. M. Effect of Surface Hydrophobicity on Adsorption and Relaxation Kinetics of Albumin and Fibrinogen: Single-Species and Competitive Behavior. *Langmuir* **2001**, *17*, 3006−3016.
(24) Ładniak, A.; Jurak, M.; Wiącek, A. E. Langmuir Monolayer Study of Phospholipid DPPC on the Titanium Dioxide−Chitosan−Hyaluronic Acid Subphases. *Adsorption* **2019**, *25*, 469−476.
(25) Jurak, M.; Mroczka, R.; Łopucki, R.; Wiącek, A. E. Structure and Wettability of Heterogeneous Monomolecular Films of Phospholipids with Cholesterol or Lauryl Gallate. *Appl. Surf. Sci.* **2019**, *493*, 1021−1031.
(26) Ładniak, A.; Jurak, M.; Wiacek, A. E. Effect of Chitosan, Hyaluronic Acid and/or Titanium Dioxide on the Physicochemical Characteristic of Phospholipid Film/Glass Surface. *Physicochem. Probl. Miner. Process.* **2019**, *55*, 1535−1548.
(27) Przykaza, K.; Jurak, M.; Wiącek, A. E.; Mroczka, R. Characteristics of Hybrid Chitosan/Phospholipid-Sterol, Peptide Coatings on Plasma Activated PEEK Polymer. *Mater. Sci. Eng., C* **2021**, *120*, 111658.
(28) Caseli, L. Enzymes Immobilized in Langmuir-Blodgett Films: Why Determining the Surface Properties in Langmuir Monolayer Is Important? *An. Acad. Bras. Cienc.* **2018**, *90*, 631−644.
(29) Tripp, B. C.; Magda, J. J.; Andrade, J. D. Adsorption of Globular Proteins at the Air/Water Interface as Measured via Dynamic Surface Tension: Concentration Dependence, Mass-Transfer Considerations, and Adsorption Kinetics. *J. Colloid Interface Sci.* **1995**, *173*, 16−27.
(30) Ward, A. F. H.; Tordai, L. Time-Dependence of Boundary Tensions of Solutions I. The Role of Diffusion in Time-Effects. *J. Chem. Phys.* **1946**, *14*, 453−461.
(31) Damodaran, S.; Song, K. B. Kinetics of Adsorption of Proteins at Interfaces: Role of Protein Conformation in Diffusional Adsorption. *Biochim. Biophys. Acta, Protein Struct. Mol. Enzymol.* **1988**, *954*, 253−264.
(32) Cho, D.; Narsimhan, G.; Franses, E. I. Adsorption Dynamics of Native and Alkylated Derivatives of Bovine Serum Albumin at Air−Water Interfaces. *J. Colloid Interface Sci.* **1996**, *178*, 348−357.
(33) Cho, D.; Cornec, M. A. A Kinetic Study on the Adsorptionof Compact, Water-Soluble Proteins onto Aqueous Surfaces. *Bull. Korean Chem. Soc.* **1999**, *20*, 999−1004.
(34) MacRitchie, F. Adsorption of Biopolymers. *Colloids Surf., A* **1993**, *76*, 159−166.
(35) Ahmed, I.; Haque, A.; Bhattacharyya, S.; Patra, P.; Plaisier, J. R.; Perissinotto, F.; Bal, J. K. Vitamin C/Stearic Acid Hybrid Monolayer Adsorption at Air−Water and Air−Solid Interfaces. *ACS Omega* **2018**, *3*, 15789−15798.
(36) Wang, S. T.; Fukuto, M.; Yang, L. In Situ X-Ray Reflectivity Studies on the Formation of Substrate-Supported Phospholipid Bilayers and Monolayers. *Phys. Rev. E: Stat. Phys., Plasmas, Fluids, Relat. Interdiscip. Top.* **2008**, *77*, 031909.
(37) Nováková, E.; Giewekemeyer, K.; Salditt, T. Structure of Two-Component Lipid Membranes on Solid Support: An x-Ray Reflectivity Study. *Phys. Rev. E: Stat. Phys., Plasmas, Fluids, Relat. Interdiscip. Top.* **2006**, *74*, 051911.
(38) Quemeneur, F.; Rinaudo, M.; Maret, G.; Pépin-Donat, B. Decoration of Lipid Vesicles by Polyelectrolytes: Mechanism and Structure. *Soft Matter* **2010**, *6*, 4471.
(39) Navon, Y.; Radavidson, H.; Putaux, J.-L.; Jean, B.; Heux, L. PH-Sensitive Interactions between Cellulose Nanocrystals and DOPC Liposomes. *Biomacromolecules* **2017**, *18*, 2918−2927.
(40) Davies, J. T. *Interfacial Phenomena*, 2nd ed.; Academic Press, 1963.
(41) Wang, S. T.; Fukuto, M.; Yang, L. In Situ X-Ray Reflectivity Studies on the Formation of Substrate-Supported Phospholipid Bilayers and Monolayers. *Phys. Rev. E: Stat. Phys., Plasmas, Fluids, Relat. Interdiscip. Top.* **2008**, *77*, 031909.
(42) Bal, J. K.; Das, N.; Mathur, T.; Plaisier, J. R.; Thomas, S. Physicochemical Properties of a Bi-Aromatic Heterocyclic-Azo/BSA Hybrid System at the Air−Water Interface. *ACS Omega* **2022**, *7*, 14031−14044.
(43) Schwenke, K. D. Charles Tanford: The Hydrophobic Effect: Formation of Micelles and Biological Membranes. 200 Seiten, Zahlreiche Abb. Und Tab., John Wiley & Sons, New York, London, Sydney, Toronto 1973. Preis: 7,90 £. *Food* **1976**, *20*, 449.
(44) Rodríguez Niño, M. R.; Lucero, A.; Rodríguez Patino, J. M. Relaxation Phenomena in Phospholipid Monolayers at the Air-Water Interface. *Colloids Surf., A* **2008**, *320*, 260−270.
(45) Rodriguezpatino, J.; Caro, A.; Rodrigueznino, M.; Mackie, A.; Gunning, A.; Morris, V. Some Implications of Nanoscience in Food Dispersion Formulations Containing Phospholipids as Emulsifiers. *Food Chem.* **2007**, *102*, 532−541.
(46) Pogorzelski, S. J.; Kogut, A. D. Static and Dynamic Properties of Surfactant Films on Natural Waters. *Oceanologia* **2001**, *43*, 223−246.
(47) Herskovits, T. T.; Harrington, J. P. Solution Studies of the Nucleic Acid Bases and Related Model Compounds. Solubility in Aqueous Alcohol and Glycol Solutions. *Biochemistry* **1972**, *11*, 4800−4811.
(48) Irving, J. T. A Histological Stain for Newly Calcified Tissues. *Nature* **1958**, *181*, 704−705.
(49) Gew, L. T.; Misran, M. Albumin-Fatty Acid Interactions at Monolayer Interface. *Nanoscale Res. Lett.* **2014**, *9*, 218.

https://doi.org/10.1021/acsomega.3c02909
ACS Omega 2023, 8, 30199−30212

(50) Zhang, A.; Jaffrezic-Renault, N.; Wan, J.; Hou, Y.; Chovelon, J.-M. Optimization of the Mixed Urease/Amphiphile Langmuir−Blodgett Film and Its Application for Biosensor Development. *Mater. Sci. Eng., C* **2002**, *21*, 91−96.
(51) Caseli, L.; Crespilho, F. N.; Nobre, T. M.; Zaniquelli, M. E. D.; Zucolotto, V.; Oliveira, O. N. Using Phospholipid Langmuir and Langmuir−Blodgett Films as Matrix for Urease Immobilization. *J. Colloid Interface Sci.* **2008**, *319*, 100−108.
(52) Ahmed, I.; Dildar, L.; Haque, A.; Patra, P.; Mukhopadhyay, M.; Hazra, S.; Kulkarni, M.; Thomas, S.; Plaisier, J. R.; Dutta, S. B.; Bal, J. K. Chitosan-Fatty Acid Interaction Mediated Growth of Langmuir Monolayer and Langmuir-Blodgett Films. *J. Colloid Interface Sci.* **2018**, *514*, 433−442.
(53) Sankaranarayanan, K.; Dhathathreyan, A.; Krägel, J.; Miller, R. Interfacial Viscoelasticity of Myoglobin at Air/Water and Air/Solution Interfaces: Role of Folding and Clustering. *J. Phys. Chem. B* **2012**, *116*, 895−902.
(54) Goodrich, F. C. *Proceedings of 2nd International Congress on Surface Activity*, 1957; p m33.
(55) Moriyama, Y.; Takeda, K. Critical Temperature of Secondary Structural Change of Myoglobin in Thermal Denaturation up to 130 °C and Effect of Sodium Dodecyl Sulfate on the Change. *J. Phys. Chem. B* **2010**, *114*, 2430−2434.
(56) Wierenga, P. A. *Basics of Macroscopic Properties of Adsorbed Protein Layers, Formed at Air-Water Interfaces, Based on Molecular Parameters*; Wageningen University and Research, 2005.
(57) Teschke, O.; de Souza, E. F. Measurements of Long-Range Attractive Forces between Hydrophobic Surfaces and Atomic Force Microscopy Tips. *Chem. Phys. Lett.* **2003**, *375*, 540−546.
(58) Zoungrana, T.; Findenegg, G. H.; Norde, W. Structure, Stability, and Activity of Adsorbed Enzymes. *J. Colloid Interface Sci.* **1997**, *190*, 437−448.
(59) Craig, V. S. J.; Ninham, B. W.; Pashley, R. M. Study of the Long-Range Hydrophobic Attraction in Concentrated Salt Solutions and Its Implications for Electrostatic Models. *Langmuir* **1998**, *14*, 3326−3332.
(60) Wood, J.; Sharma, R. How Long Is the Long-Range Hydrophobic Attraction? *Langmuir* **1995**, *11*, 4797−4802.
(61) Kundu, S.; Matsuoka, H.; Seto, H. Zwitterionic Lipid (DPPC)-Protein (BSA) Complexes at the Air-Water Interface. *Colloids Surf., B* **2012**, *93*, 215−218.
(62) Palaniappan, V.; Bocian, D. F. Acid-Induced Transformations of Myoglobin. Characterization of a New Equilibrium Heme-Pocket Intermediate. *Biochemistry* **1994**, *33*, 14264−14274.
(63) Zhu, L.; Brewer, M. Effects of PH and Temperature on Metmyoglobin Solubility in a Model System. *Meat Sci.* **2002**, *61*, 419−424.
(64) Postel, C.; Abillon, O.; Desbat, B. Structure and Denaturation of Adsorbed Lysozyme at the Air−Water Interface. *J. Colloid Interface Sci.* **2003**, *266*, 74−81.
(65) Malmsten, M. Formation of Adsorbed Protein Layers. *J. Colloid Interface Sci.* **1998**, *207*, 186−199.
(66) Graham, D.; Phillips, M. Proteins at Liquid Interfaces. *J. Colloid Interface Sci.* **1979**, *70*, 403−414.
(67) Bismuto, E.; Colonna, G.; Irace, G. Unfolding Pathway of Myoglobin. Evidence for a Multistate Process. *Biochemistry* **1983**, *22*, 4165−4170.
(68) Birdi, K. Spread Monolayer Films of Proteins at the Air—Water Interface. *J. Colloid Interface Sci.* **1973**, *43*, 545−547.
(69) Langmuir, I.; Schaefer, V. J. Activities of Urease and Pepsin Monolayers. *J. Am. Chem. Soc.* **1938**, *60*, 1351−1360.

https://doi.org/10.1021/acsomega.3c02909
ACS Omega 2023, 8, 30199−30212